Geometric Predictions of Scaling at Tricritical Points*

Alex Hankey, H. Eugene Stanley, and T. S. Chang†
Physics Department, Massachusetts Institute of Technology, Cambridge, Massachusetts 02139
(Received 24 May 1972)

The shapes of the three critical lines meeting at a tricritical point are discussed in the light of the homogeneity hypothesis. We give a complete listing of possible shapes consistent with scaling. Certain possible geometries are thereby shown to be *inconsistent* with scaling. Application of these ideas to the crossover regions is shown to considerably simplify the "metric problem" posed by Riedel.

Riedel[1] has recently proposed a theory of scaling for tricritical points (TCP's). His work treats scaling in the two-dimensional "physical plane" (his g-T plane) near the TCP, instead of in the full three-dimensional space which, as Griffiths and Wheeler[2,3] pointed out, is needed to better comprehend the thermodynamics of complex systems.

This paper shows how the geometry of curves and surfaces of singularities at the TCP is determined by the equation of scaling there; in particular, it is shown that certain shapes of critical lines at the TCP are *inconsistent with scaling*. Also, we make predictions about the "wings" (c.f., Fig. 1). These are of interest because anomalous behavior of some thermodynamic functions may be expected in the H-T plane at points close to the wings.

Predictions of scaling for the lines L_1, L_2, and L_3.—At each point P on a critical line L_j (cf. Fig. 1), a triad of vectors $x_i(L_j)$ can be established. The first, $x_1(L_j)$, points out of the coexistence surface (CXS) in a strong direction (S); the second, $x_2(L_j)$, a weak direction (W), points out of the critical line but is in the plane of the CXS; the third is tangent to the critical line, and we call this an independent direction (I). $x_1(L_j)$ and $x_2(L_j)$ can be uniquely chosen to be orthogonal to $x_3(L_j)$ and to each other. As the point P moves to the TCP, the triad $[x_1(L_j), x_2(L_j), x_3(L_j)]$ attains a limiting orientation.

It is shown below that unless a degeneracy occurs, the scaling hypothesis implies that the orientation of these three triads is parallel, in the sense that *each* member of a particular triad possesses a parallel counterpart in each of the other triads. These three directions will be the principal directions of scaling about the TCP. We denote these three[4] directions by $\bar{x}_j \equiv \lim(P \to \mathrm{TCP}) x_j(L_1)$ (cf. Fig. 1).

The scaling hypothesis about tricritical points can be made in such a fashion that all the variables $\bar{x}_1$, $\bar{x}_2$, $\bar{x}_3$ are treated on an equal footing (i.e., we introduce a "scaling power" $\bar{a}_j$ for each direction): The singular part of the Gibbs potential is asymptotically a generalized homogeneous function,[5]

$$G(\lambda^{\bar{a}_1}\bar{x}_1, \lambda^{\bar{a}_2}x_2, \lambda^{\bar{a}_3}\bar{x}_3) = \lambda G(\bar{x}_1, \bar{x}_2, \bar{x}_3). \quad (1)$$

All tricritical point exponents are derivable in terms of the three scaling powers $\bar{a}_1$, $\bar{a}_2$, $\bar{a}_3$.

The scaling hypothesis (1) predicts the geometric shape of the three critical lines, and this may be seen as follows. If the function G possesses a singularity at a particular point $Q \equiv (\bar{x}_1, \bar{x}_2, \bar{x}_3)$, then by (1) it must also possess a singularity at the point $Q' \equiv (\lambda^{\bar{a}_1}\bar{x}_1, \lambda^{\bar{a}_2}\bar{x}_2, \lambda^{\bar{a}_3}\bar{x}_3)$. Therefore, the three critical lines must possess a parametric representation in the coordinate frame

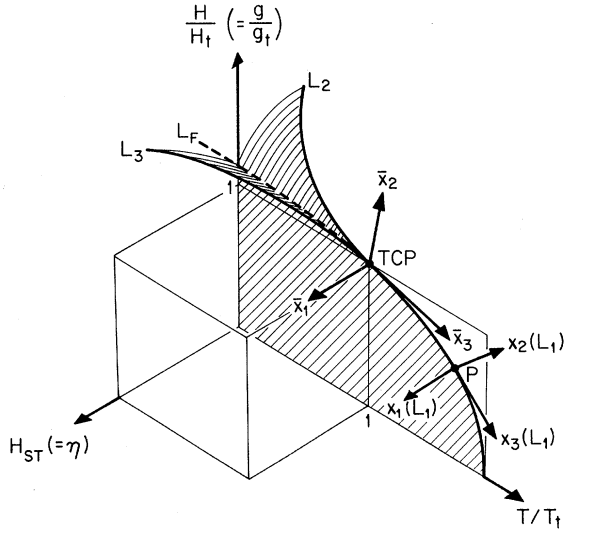

FIG. 1. The wings and the physical plane for Case I. The axes are indicated for magnets, with the more general terminology (Ref. 1) in brackets. The coexistence surfaces are indicated by shading. The wings are bounded by L_2, L_3, and the CXS in the physical plane by L_1. At a point P on L_1, the three principal directions of ordinary scaling are indicated. These assume the limiting orientations $(\bar{x}_1, \bar{x}_2, \bar{x}_3)$ at the TCP.

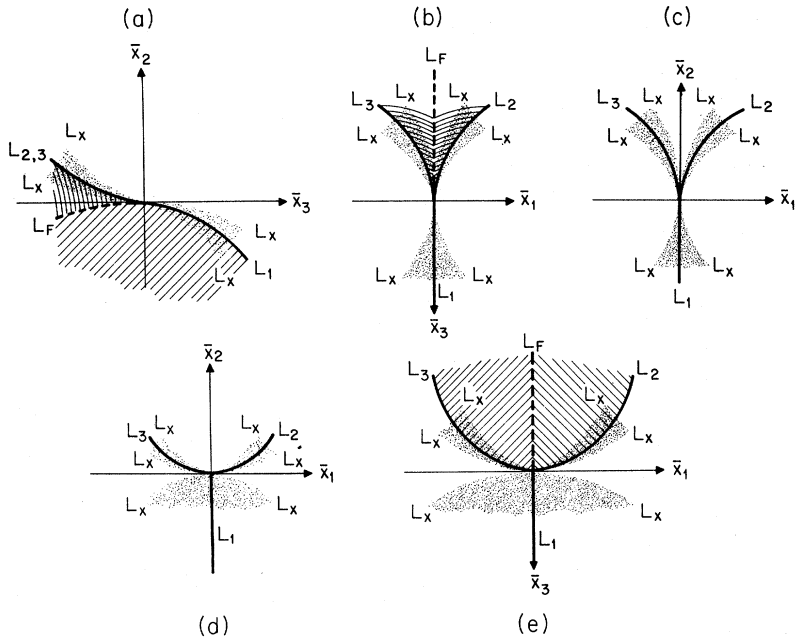

FIG. 2. Projections of the region near the TCP, parallel to one of the axes $\bar{x}_j$ of TCP scaling, onto the plane formed by the other two axes. This is for nondegenerate cases. The wings and the CXS in the physical plane are shaded. The speckled regions indicate where the scaling about the lines should be valid; their boundaries, denoted by L_X, are the projections onto the planes of the edges of the regions in the *full* three-dimensional space. (a) Projection onto $\bar{x}_2,\bar{x}_3$ plane. (b) Projection onto the $\bar{x}_1,\bar{x}_3$ plane for $\bar{a}_1 > \bar{a}_3$. (c) Projection onto the $\bar{x}_1,\bar{x}_2$ plane for $\bar{a}_1 > \bar{a}_2$. Note the wings cannot now be seen. (d) Projection onto the $\bar{x}_1,\bar{x}_2$ plane for $\bar{a}_1 < \bar{a}_2$. (e) Projection onto the $\bar{x}_1$, $\bar{x}_3$ plane for $\bar{a}_1 < \bar{a}_3$.

$(\bar{x}_1,\bar{x}_2,\bar{x}_3)$ of the form

$$L_j \equiv (A_j r^{\bar{a}_1}, B_j r^{\bar{a}_2}, C_j r^{\bar{a}_3}). \tag{2}$$

Using the facts that L_1 lies in the physical plane and L_2, L_3 are symmetric about it, we find $A_1 = 0$, $A_3 = -A_2$, $B_2 = B_3$, and $C_2 = C_3$. Thus L_1 approaches the TCP parallel to the axis corresponding to the lesser of $\bar{a}_2$ and $\bar{a}_3$. Since this axis has been defined to be the $\bar{x}_3$ axis we conclude that

$$\bar{a}_2 \geq \bar{a}_3. \tag{3}$$

In the case that (3) is an equality, $B_1 = 0$. Similarly, (2) shows that the lines L_2, L_3 approach the TCP parallel to the $\bar{x}_k$ axis, where k is such that $\bar{a}_k$ is the minimum of $\bar{a}_1$, $\bar{a}_2$, and $\bar{a}_3$.

The general shapes of the L_j at the TCP are determined by the relative magnitudes of $\bar{a}_1$, $\bar{a}_2$, and $\bar{a}_3$. The inequality (3) reduces the number of possible orderings from six to three. In addition there are *degenerate* cases where two $\bar{a}_j$ are equal. Ignoring these for the moment, the three nondegenerate cases are (I) $\bar{a}_1 > \bar{a}_2 > \bar{a}_3$, (II) $\bar{a}_2 > \bar{a}_1 > \bar{a}_3$, and (III) $\bar{a}_2 > \bar{a}_3 > \bar{a}_1$.

A general prediction of scaling can be made initially: When the lines L_1, L_2, and L_3 are viewed in projection along the $\bar{x}_1$ axis, they must all approach the TCP along the $\bar{x}_3$ direction [c.f. Fig. 2(a)] *or* else $\bar{a}_2 = \bar{a}_3$ (which can be checked by exponent comparison[6]).

Case I, $\bar{a}_1 > \bar{a}_2 > \bar{a}_3$: Because $\bar{a}_3$ is smallest, the lines L_2, L_3 approach the TCP along the $\bar{x}_3$ axis [cf. Figs. 2(b) and 2(c)]. This case should produce interesting effects in the physical plane, since the lines L_2, L_3 remain close to the physical plane as they move away from the TCP. The Blume-Emery-Griffiths model[7] is of this type. The orientation of the coexistence surfaces forming the wings is given in Table I.[8]

TABLE I. Properties of the directions $(\bar{x}_1,\bar{x}_2,\bar{x}_3)$ for the *nondegenerate* cases. Here S denotes the strong direction, W the weak direction, and I the independent direction.

	Case I			Case II			Case III		
	L_1	L_2	L_3	L_1	L_2	L_3	L_1	L_2	L_3
$\bar{x}_1$	S	S	S	S	W	W	S	I	I
$\bar{x}_2$	W	W	W	W	S	S	W	S	S
$\bar{x}_3$	I	I	I	I	I	I	I	W	W

Case II, $\bar{a}_2 > \bar{a}_1 > \bar{a}_3$: In this case the projection along the $\bar{x}_2$ axis is the same as in Fig. 2(b) (since $\bar{a}_1 > \bar{a}_3$ as in Case I), while that along the $\bar{x}_3$ axis is shown in Fig. 2(d) which shows that the limiting orientation of the wings is now perpendicular to the physical plane.[8] The properties of $(\bar{x}_1, \bar{x}_2, \bar{x}_3)$ are summarized in Table I.

Case III, $\bar{a}_2 > \bar{a}_3 > \bar{a}_1$: Here the projection along $\bar{x}_2$ is given in Fig. 2(e), while the projection along $\bar{x}_3$ is the same as Fig. 2(d) (since $\bar{a}_2 > \bar{a}_1$ as in Case II). In this case not only do the two wings meet the physical plane perpendicularly [cf. Fig. 2(d)] but the line L_2-L_3 also intersects the line L_1 perpendicularly because $\bar{a}_3 > \bar{a}_1$ [cf. Fig. 2(e)]. The properties of the $\bar{x}_j$ are summarized in Table I. Finally there is the possibility that two of the powers $\bar{a}_j$ are equal, for which Eq. (2) allows the lines L_1, L_2, L_3 to meet at angles other than multiples of 90°.[9]

Case IV, $\bar{a}_1 = \bar{a}_2 > \bar{a}_3$: There is degeneracy between $\bar{x}_1$ and $\bar{x}_2$. The projection along $\bar{x}_2$ is the same as in Fig. 2(b) (since $\bar{a}_1 > \bar{a}_3$), while the projection along $\bar{x}_3$ is given in Fig. 3(a); $\bar{x}_1$ and $\bar{x}_2$ are not *both strong* for the wings (since both are out of the critical line and CXS) and an appropriate combination of $\bar{x}_1$ and $\bar{x}_2$ must be found to obtain a weak direction.

Case V, $\bar{a}_2 > \bar{a}_3 = \bar{a}_1$: Here there is degeneracy between $\bar{x}_1$ and $\bar{x}_3$. The strong and weak directions are the same as in Table I, Case II, but appropriate combinations of $\bar{x}_1$ and $\bar{x}_3$ form the independent directions at the TCP. The projection along $\bar{x}_2$ is given in Fig. 3(b).

Degeneracy between $\bar{a}_2$ and $\bar{a}_3$ and "full degeneracy" $(\bar{a}_1 = \bar{a}_2 = \bar{a}_3)$ can be treated similarly.

This case-by-case analysis shows that only a limited set of geometries is possible at the TCP. E.g., the lines L_2, L_3 can *never* approach the TCP along the $\bar{x}_2$ axis, and any system with this geometry would violate the scaling hypothesis (1).

Scaling for the crossover lines L_X.—When two *different* scaling equations hold in adjacent regions, there are ill-defined "boundaries" between these regions.[1] On these boundaries the scaling behavior "crosses over" from one type to another (e.g., tricritical to critical line). The positions of these boundaries have previously been a matter of question.[1]

If the equation of homogeneity (1) is valid, then the boundaries of the regions of validity of the scaling laws should also be parametrized. This is because the boundaries will be determined by inequalities between $\bar{x}_2$ and $\bar{x}_3$; however (1) tells us that the quantities of significance near the

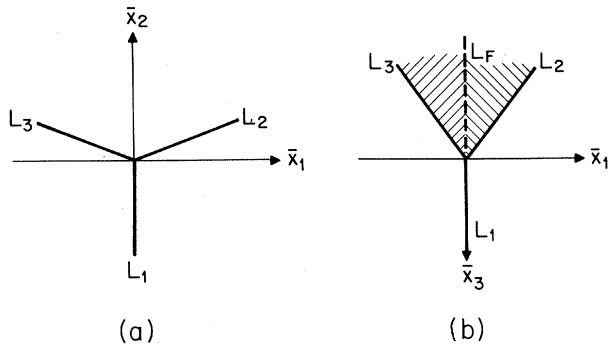

FIG. 3. The same as Fig. 2, but for the *degenerate* cases. (a) Case IV, $\bar{a}_1 = \bar{a}_2$, (b) Case V, $\bar{a}_1 = \bar{a}_3$. Since the $L_j \rightarrow$ TCP with non-zero slope, the slopes of the L_X are undetermined.

TCP are not $\bar{x}_2$ and $\bar{x}_3$, but $\bar{x}_2^{1/\bar{a}_2}$ and $\bar{x}_3^{1/\bar{a}_3}$. Hence any inequalities governing the scaling regions will be relations between these quantities, and we will therefore expect the boundaries to be parametrized in the same fashion as the lines of singularities, Eq. (2). This will give their general shapes once the relative magnitudes of $\bar{a}_1$, $\bar{a}_2$, and $\bar{a}_3$ are known (from the positions of the wings or otherwise).

To give a feeling for the inequalities that arise between the quantities $\bar{x}_1^{1/\bar{a}_1}$, $\bar{x}_2^{1/\bar{a}_2}$, and $\bar{x}_3^{1/\bar{a}_3}$, we offer an example of a model function for the susceptibility which obeys scaling and describes the behavior in the physical $(\bar{x}_2$-$\bar{x}_3)$ plane for $T > T_t$,

$$\chi = A(\bar{x}_2 + B\bar{x}_3^{1/\varphi})^{-(\bar{\gamma}-\gamma)}(\bar{x}_2 - k\bar{x}_3^{1/\varphi})^{-\gamma}; \qquad (4)$$

χ has a line of singularities L_1 at $\bar{x}_2 = k\bar{x}_3^{1/\varphi}$, and comparison with the last section shows that $\varphi \equiv \bar{a}_3/\bar{a}_2$. First note that if $\bar{x}_3 = 0$, $\chi = A\bar{x}_2^{-\bar{\gamma}}$, so that $\bar{\gamma}$ is the "TCP exponent." Next, if $\bar{x}_3 > 0$, and we let $\bar{x}_2 - k\bar{x}_3^{1/\varphi} \equiv \epsilon$, then

$$\chi = A[(B+k)\bar{x}_3^{1/\varphi} + \epsilon]^{-(\bar{\gamma}-\gamma)}\epsilon^{-\gamma}. \qquad (5)$$

This function has two sorts of behavior depending on the relative magnitudes of ϵ and $(B+k)\bar{x}_3^{1/\varphi}$. This gives inequalities of the form suggested, since the quantities related are $\bar{x}_2$ and $\bar{x}_3^{\bar{a}_2/\bar{a}_3}$. In fact for $\epsilon \ll (B+k)\bar{x}_3^{1/\varphi}$, χ diverges with exponent γ as $\epsilon \rightarrow 0$. For $\epsilon \gg (B+k)\bar{x}_3^{1/\varphi}$, it diverges as $\epsilon^{-\bar{\gamma}}$. The equation of the crossover line is therefore given by

$$\bar{x}_2 \cong (B+2k)\bar{x}_3^{1/\varphi}, \qquad (6)$$

and this possesses the same "scaling-determined" geometric behavior as the line L_1. This reasoning determines the shapes of all the crossover

lines L_X.

Restricting our attention to the physical plane considered by Riedel, it is clear that the crossover lines must approach the TCP along the $\bar{x}_3$ axis if (3) is *not* an equality. Since the domain in which thermodynamic functions satisfy TCP scaling is only a limited region, and since near the TCP, the position of the crossover lines L_X is close to the $\bar{x}_3$ direction, the lines L_X are fairly accurately placed. The "metric problem"[1] is thus considerably simplified and may even be effectively disregarded in *nondegenerate* cases.

The Blume-Emery-Griffiths (BEG) model.[7]—An example for which the wings' positions are known and for which we can solve for the relative values of $\bar{a}_1$, $\bar{a}_2$, and $\bar{a}_3$ is the BEG spin model for He^3-He^4 mixtures, which has been treated extensively by mean-field theory.[7] We find that for this model, $\bar{a}_1:\bar{a}_2:\bar{a}_3 = 5:4:2$. Hence, the mean-field-theory solution of the BEG model exemplifies Case I, $\bar{a}_1 > \bar{a}_2 > a_3$.

Critical-point exponents in terms of $\bar{a}_j$.—These may be obtained by appropriate differentiation of Eq. (1). E.g., $\chi \sim (T - T_t)^{-\bar{\gamma}}$ with $-\bar{\gamma} = (1 - 2\bar{a}_2)/\bar{a}_2$, and $\bar{a}_2$ is determined *uniquely* by $\bar{\gamma}$. A number of "physical-plane exponents" are expressible in terms of $\bar{a}_2$, $\bar{a}_3$. E.g., for the Ising metamagnet $FeCl_2$,[10] $\bar{\gamma} \cong \frac{1}{2}$ and $\varphi \equiv \bar{a}_3/\bar{a}_2 \cong \frac{1}{2}$; hence $\bar{a}_2 \cong \frac{2}{3}$, $\bar{a}_3 \cong \frac{1}{3}$. Knowledge of the behavior of M_{st} or χ_{st} will yield $\bar{a}_1$.

We wish to thank F. Harbus for useful discussions.

* Portions of this work were presented at the March 1972 meeting of the American Physical Society; see Bull. Amer. Phys. Soc. 17, 277 (1972). Supported by the Laboratory for Nuclear Science (Massachusetts Institute of Technology), the National Science Foundation, the U. S. Office of Naval Research, the U. S. Office of Scientific Research, and the National Aeronautics and Space Administration.

†Permanent address: Riddick Laboratories, North Carolina State University, Raleigh, N. C. 27607.

[1]E. K. Riedel, Phys. Rev. Lett. 28, 675 (1972).

[2]R. B. Griffiths, Phys. Rev. Lett. 24, 715 (1970).

[3]R. B. Griffiths and J. C. Wheeler, Phys. Rev. A 2, 1047 (1970).

[4]The reader may have some difficulty at this point in making correspondence between the present notation and that of Ref. 1. There is no counterpart to $\bar{x}_1$ because the equations of Ref. 1 were restricted to $\bar{x}_1 = 0$. The variables $\bar{x}_2, \bar{x}_3$ are denoted by μ_1, μ_2, respectively, in Ref. 1.

[5]For a systematic application of generalized homogeneous functions to scaling, see A. Hankey and H. E. Stanley, Phys. Rev. B (to be published).

[6]For example, $\varphi = \bar{a}_3/\bar{a}_2$, $-\bar{\gamma} = (1 - 2\bar{a}_2)/\bar{a}_2$, $-\bar{\gamma}_{st} = (1 - 2\bar{a}_1)/a_2$, $\bar{\beta}_{st} = (1 - \bar{a}_1)/\bar{a}_2$.

[7]M. Blume, V. J. Emery, and R. B. Griffiths, Phys. Rev. A 4, 1071 (1971).

[8]There is one exceptional case which is not treated here.

[9]In the event that one finds a model system displaying this behavior, then one must test the possibility that two scaling powers are equal (Ref. 6); otherwise the scaling hypothesis (1) is *invalid* for this model.

[10]F. Harbus, private communication. See also F. Harbus and H. E. Stanley, Phys. Rev. Lett. 29, 58 (1972).

Q-Switch and Polarization Domains in Antiferromagnetic Chromium Observed with Neutron-Diffraction Topography

Masami Ando and Sukeaki Hosoya
Institute for Solid State Physics, University of Tokyo, Roppongi, Minato-ku, Tokyo, Japan
(Received 17 March 1972)

The *Q*-switch and polarization domain configurations in a nearly perfect Cr single crystal has been directly observed by neutron-diffraction topography in the AF_1 and AF_2 phases. The size of the domains proves to be as large as 10^{-3} to 10^{-2} cm^3 in either phase. As far as the present observation is concerned, each domain in the AF_2 phase splits into domains in the AF_1 phase, with two possible polarizations of the transverse spin-density wave.

In a previous paper[1] it was reported that the *Q*-switch domain boundaries in antiferromagnetic Cr in the AF_2 phase at 78 K were observed by means of x-ray double-crystal topography, using the slight deviation from cubic symmetry. In the present paper, unambiguous direct observations are reported on *Q*-switch and polarization domains by the use of new neutron topography. As is well known, there can be three kinds of domains in the AF_2 phase and six in the AF_1, and each of them gives independent neutron satellite diffractions at different positions in the recipro-